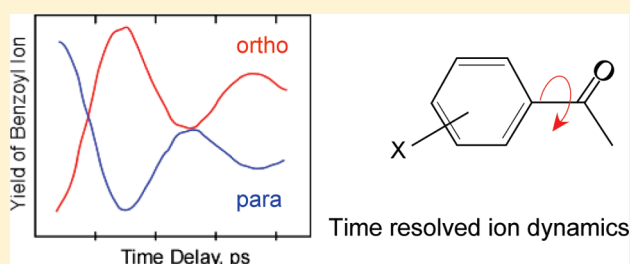


Photodissociation Dynamics of Acetophenone and Its Derivatives with Intense Nonresonant Femtosecond Pulses

Xin Zhu,[†] Vadim V. Lozovoy,[†] Jay D. Shah,[†] and Marcos Dantus^{*,†,‡}[†]Department of Chemistry and [‡]Department of Physics and Astronomy, Michigan State University, East Lansing, Michigan 48824, United States**S** Supporting Information

ABSTRACT: Recent work from our group (Lozovoy, V. V.; Zhu, X.; Gunaratne, T. C.; Harris, D. A.; Shane, J. C.; Dantus, M. J. *Phys. Chem. A* **2008**, *112*, 3789) using shaped nonresonant femtosecond pulses to ionize and fragment polyatomic molecules indicated that pulse duration is the most important parameter for controlling the relative yield of different fragment ions. Here we explore the time-resolved dynamics that ensue following the interaction of the molecules with a strong 10^{15} W/cm² nonresonant near-infrared laser field. The data reveal that most of the fragmentation processes occur well after ionization.

The molecular dynamics are followed in the 10^{-14} – 10^{-10} s time scale. Studies carried out on acetophenone derivatives are used to assign the observed modulation in the benzoyl product ion yield, which is found to correlate with further ionization and fragmentation through electronic coordination. The resulting experimental data, together with photoelectron spectra and the electron-ionization mass spectra of these compounds, allow us to propose ladder switching processes taking place in this family of compounds which regulate the different fragment ions observed. This analysis sheds light on how pulse duration influences the yield of different fragment ions.



INTRODUCTION

It has been over two decades since ultrafast lasers were first used to explore the photodissociation dynamics of molecules. During this time, important lessons have been learned about direct and indirect bond breakage, curve crossing dynamics, and dynamics over saddle points. Over a decade ago, some interest shifted from probing the dynamics to controlling the dynamics. Of particular interest were studies in which an intense nonresonant laser field is shaped prior to interacting with isolated molecules, and the subsequent yield of fragment ions, detected using a mass spectrometer, was found to vary according to the phase and amplitude of the shaped laser pulses. Recently, experimental evidence indicates that pulse duration can account for the majority of the changes in fragmentation observed.^{1–6} Here, we turn our attention to the dynamics occurring soon after isolated molecules interact with an intense nonresonant laser field. Our study reveals dynamics taking place over a range of four orders of magnitude in time, and these provide information about how molecules interact with intense laser fields and how pulse shaping influences the yield of different fragment ions.

Early femtosecond photodissociation dynamics studies were carried out using a pump laser that was resonant with an electronic potential energy surface (PES), and the dynamics occurring on the PES were subsequently probed by a probe laser pulse tuned to detect the photofragments.^{7–9} Since the early days it was noted that femtosecond lasers, even when not resonant with an electronic transition, would be able to cause

excitation, fragmentation, and ionization. A distinction was made between long pulse excitation, where the process could be characterized by multiphoton transitions, and short pulse excitation, where the process was characterized by fast, single optical cycle, field ionization followed by fragmentation. The former process became known as ladder switching to indicate that photodissociation takes place at a comparable rate with transitions among upper excited states.^{10,11}

Direct ultrafast excitation to selected PES allowed direct probing of wave packet dynamics. Bound and quasibound states arising from the crossing of electronic states led to the observation of coherent oscillations. Extrapolating from the early studies, one would expect that a shaped pulse could be used to time a number of discrete transitions among two or more PES in order to direct the photodissociation reaction and control the product formation. Control of a wave packet requires a collection of sub-50 fs pulses at a number of different wavelengths in the 260–532 nm spectral region. A laser source capable of creating three or more pulses by pulse shaping a single input pulse in the UV–vis wavelength range is still outside of present technical capabilities, although significant progress is being made on shaped UV sources and their use for controlling chemical reactions.^{12–14} The widely available near-IR femtosecond shaped sources have

Received: April 1, 2010

Revised: November 18, 2010

Published: January 12, 2011

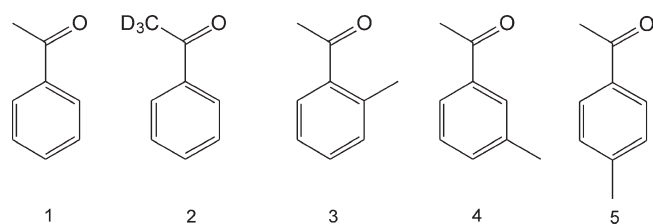


Figure 1. Structures of the acetophenone, d_3 -acetophenone, and three methyl-acetophenone isomers: (1) acetophenone, (2) β,β,β -deuterated acetophenone, (3) 2-methyl-acetophenone, (4) 3-methyl-acetophenone, and (5) 4-methyl-acetophenone.

already inspired numerous laser control experiments in which significant changes over product distribution have been observed.^{15,16} Efforts to explain the observed changes in the yield of different photofragments in terms of pulses timed to trigger transitions between different PES acting on the evolving localized wave packet were complicated by the lack of information about excited state potential energy surfaces, and their transition dipoles as a function of different reaction coordinates. A new interpretation of strong nonresonant photodissociation recognizes that the laser pulse causes field ionization, and the time during which the field acts on the nascent ion is more likely regulating ladder climbing and ladder switching events.¹

Here we perform a series of pump–probe experiments on acetophenone (1), partially deuterated acetophenone (2), 2-methyl-acetophenone (3), 3-methyl-acetophenone (4), and 4-methyl-acetophenone (5), as shown in Figure 1. We compare results obtained by electron ionization mass spectrometry and those obtained by femtosecond photoionization using near-IR ultrashort pulses. Those results, together with the time-resolved measurements and comparison between the different derivative compounds, allow us to propose that pulse shaping acts by controlling ladder climbing and ladder switching processes that take place during the strong-field excitation of this family of polyatomic molecules.

EXPERIMENTAL SECTION

All the experiments reported here were carried out using a time-of-flight mass spectrometer (TOFMS) with a 0.5 m field-free drift region. Sample molecules were effused through a leak valve into the chamber, where the pressure was maintained with a three stage differentially pumped system at 10^{-5} Torr during the experiments and 10^{-7} Torr within a second of closing the leak valve. Fast flow in the TOFMS ensures the sample is constantly removed and prevents the accumulation of contaminants.

The femtosecond laser system (Figure 2) consists a regeneratively amplified Ti:sapphire laser (Spitfire-Spectra Physics) seeded with a 86 MHz oscillator (KM Laboratories, 45 mm fwhm). Typical output from the amplifier is 700 $\mu\text{J}/\text{pulse}$ at 1 kHz, and centered at 800 nm. Phase distortions introduced by the laser system, all the optics, and air were compensated using a MIIPS enabled phase only pulse shaper resulting in 35 fs (fwhm) transform-limited pulses.^{17,18} The output pulses were split by a 50/50 beam splitter and spatially recombined with an adjustable delay before entering the mass spectrometer. For some experiments, a 10 cm path length water filled glass cell was placed in one of the arms to introduce $+2500 \text{ fs}^2$ linear chirp, which broadened the probe pulses to ~ 200 fs pulse duration. Neutral density filters were placed in the beam paths to adjust the laser irradiance such that energy/pulse was always the same. A further discussion

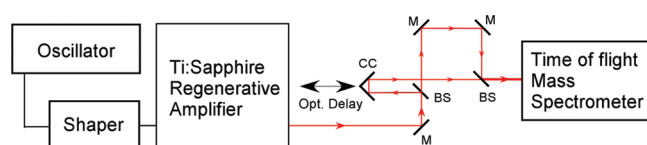


Figure 2. Schematic of the experimental setup: BS, 50/50 intensity beam splitter; M, silver coated reflective mirror; CC, corner cube.

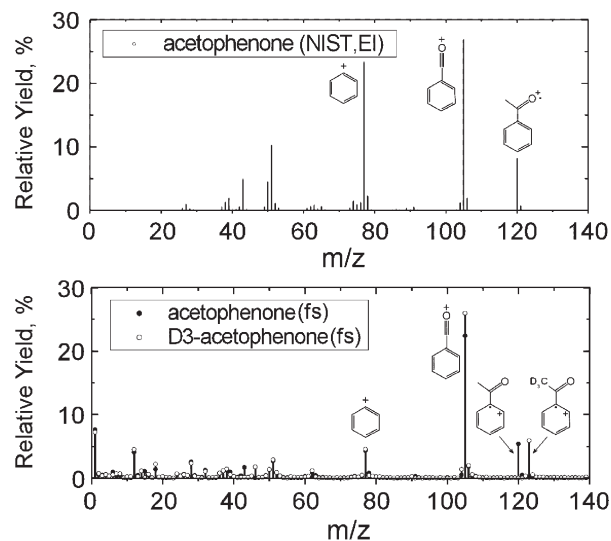


Figure 3. Top: mass spectra of acetophenone obtained by 70 eV electron ionization. Bottom: mass spectra of acetophenone and deuterated acetophenone obtained by femtosecond laser ionization.

regarding the rationale for using TL pump and a chirped probe pulse is given in the Supporting Information, and illustrated in Figure S4.

A 50 mm focal length lens was used to focus the pulses into the chamber of the mass spectrometer and cause ionization and dissociation of gas phase acetophenone molecules. The focal spot size and Rayleigh length were determined to be 6.4 and 66 μm (beam propagation ratio $M^2 = 1.5$ at the focus), respectively, using a CCD camera beam profiling system (Coherent). Typical pulse energy at the focus was attenuated to 100 $\mu\text{J}/\text{pulse}$, giving a maximum intensity of $4 \times 10^{15} \text{ W}/\text{cm}^2$ for TL pulses using the formula $I_0 = 4(\ln 2)^{1/2}W/(\tau\omega_0^2\pi^{3/2})$, where W is the pulse energy (J), τ is the time duration of the pulse(s), and ω_0 is the radius at the focus when intensity drops by $1/e^2$ (cm) (also called focal spot size). No efforts to mitigate the Gaussian intensity distribution inherent with laser excitation were needed for these experiments. The intensity distribution, also known as “volume effect”, is only relevant in this study when pump and probe pulses are overlapped in time, and results in a higher yield of ions. A further discussion regarding this topic is given in the Supporting Information and illustrated in Figure S4.

For all experiments, part of the beam (after recombination) was directed to a 50 μm type I β -BBO crystal generating the second harmonic generation (SHG) of the shaped laser pulses as an indicator of time zero and also for the purpose of monitoring laser stability.

Experimental samples of acetophenone ((Fluka >99.5%), β,β,β - d_3 -acetophenone (Aldrich >99%), 2-methyl-acetophenone (Fluka >98.0%), 3-methyl-acetophenone (Aldrich >98.0%), and

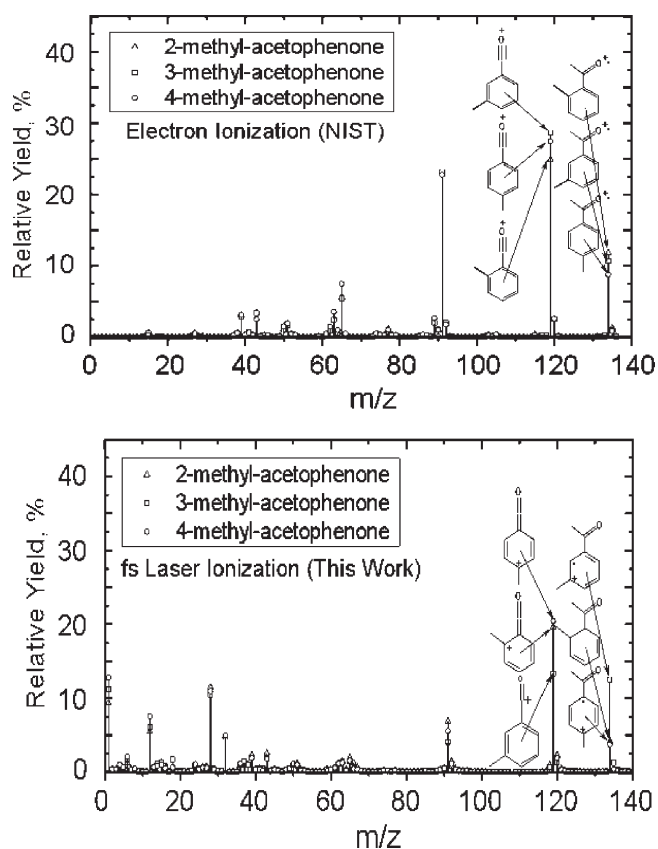


Figure 4. Mass spectra of methyl-acetophenones obtained by electron ionization (top) and femtosecond laser ionization (bottom).

4-methyl-acetophenone (Fluka >96.0%) were used without further purification.

RESULTS

Mass Spectra of Acetophenone. The mass spectra obtained for acetophenone when measured either by 70 eV electron ionization or 35 fs transform limited (800 nm) laser pulses are presented in Figure 3. The molecular ion is identified by its m/z 120. The major fragment ion species observed for both ionization methods are essentially the same. The mass spectrum of partially deuterated acetophenone (d_3) was also obtained by femtosecond excitation pulses. The only differences observed between acetophenone and d_3 -acetophenone in the bottom panel of Figure 3 are the molecular ion masses and the fragment ion with 43 and 46 m/z . This indicates that all other product ions lack the methyl group. If the methyl group remained attached, then the photo-fragments observed for partially deuterated acetophenone would have been shifted by three mass units corresponding to the three deuterium atoms in CD_3 .

Mass Spectra of Methyl-acetophenones. The mass spectra of three methyl-acetophenone isomers, with molecular ion at m/z 134, are presented in Figure 4. There is almost no difference in the fragmentation patterns of the three isomers when obtained by electron ionization. However, when femtosecond pulses are used to induce the photoionization, the molecular ion abundance of 3-methyl-acetophenone is significantly higher and its benzoyl ion abundance is significantly lower than those of the other two isomers. The reason for this difference will be discussed later.

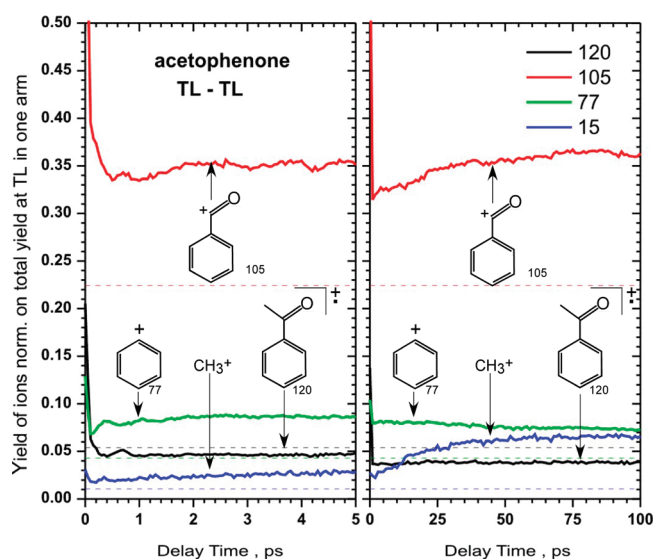


Figure 5. Yield of several major fragment ions from acetophenone plotted with respect to the time delay between (TL) pump and (TL) probe pulses. Dashed lines show yields of fragments when only one TL pulse was used.

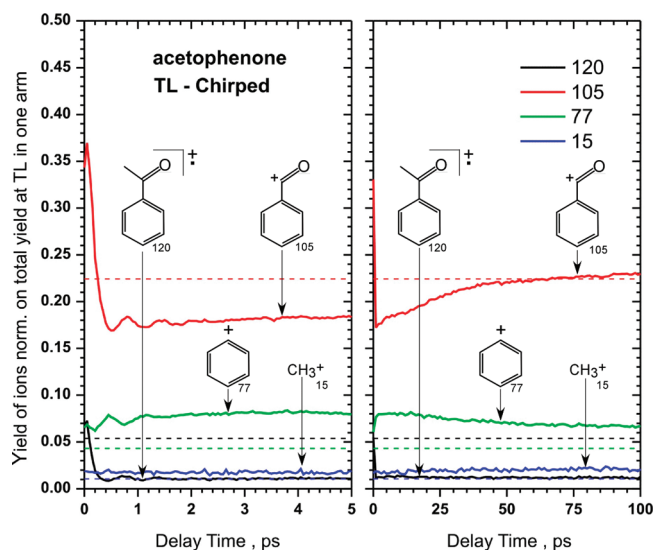


Figure 6. Yield of several major fragment ions from acetophenone plotted with respect to the time delay between (TL) pump and (chirped) probe pulses. Dashed lines show yields of fragments when only one TL pulse was used.

Pump (TL)–Probe (TL) on Acetophenone. Time-resolved photodissociation experiments of acetophenone were carried out using two 800 nm transform-limited pulses ($\tau_{\text{fwhm}} = 35$ fs) for two different time scales, -5 ps to 5 ps, and -100 ps to 100 ps. The relative yields of several major fragments including molecular ion (m/z 120), benzoyl ion (m/z 105), phenyl ion (m/z 77), and methyl ion (m/z 15) were plotted with respect to the time delay between the pump and probe pulses, as shown in Figure 5. Given that laser pulse energies were always kept the same for the pump and the probe pulses, the relative yields of the fragments are symmetric about time zero. Therefore, in Figure 5, only the results with positive time delays are shown.

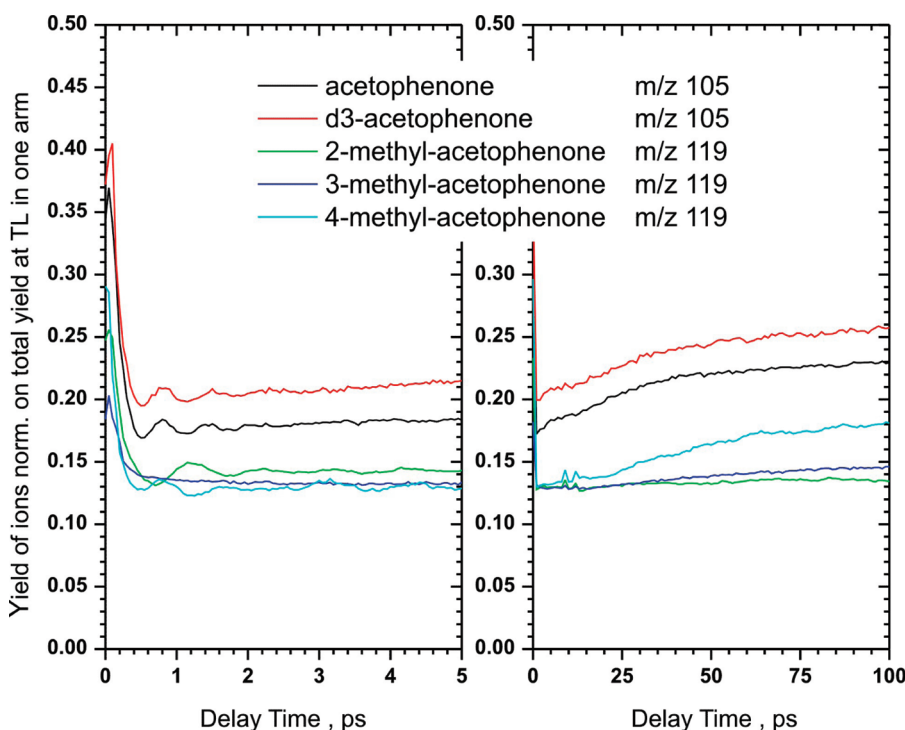


Figure 7. Yields of benzoyl ion from acetophenone, d_3 -acetophenone, and three methyl-acetophenone isomers plotted with respect to the delay between TL pump pulse and chirped probe pulse.

For all the fragment ions the maximum value was observed at time zero, and the maximum yield decayed following the cross correlation between pump and probe pulses <50 fs. The relative yields of benzoyl ion (m/z 105) and methyl ion (m/z 15), having reached a minimum at early times, increase with time delay. An exponential rise with time constant of 20.0 ± 1.6 ps and 18.5 ± 0.7 ps was measured, respectively. The relative yield of phenyl ion decreased with an exponential decay time constant of 19.6 ± 1.8 . The relative yield of the molecular ion remained almost unchanged after the first picosecond.

Pump (TL)–Probe (Chirped) on Acetophenone. Measurements were also carried out for acetophenone using a TL pump pulse followed by a $+2500$ fs² chirped probe pulse. The rationale behind these measurements was that we wanted to better understand the ~ 1 ps modulation in the ion yields. By chirping the probe beam, we ensure that it causes minimum ionization, and more importantly, because of its lower intensity, it probes a smaller volume of molecules than the TL pump laser (see Supporting Information Figure S4). Thus, the difference as a function of time is caused only by molecules that were first ionized by the pump laser. Given that the energy per pulse for both pump and probe is the same, the TL pulses have a 5.7 times higher peak intensity than the chirped pulses. When the TL pulses are used as the pump pulse, most of the molecules inside the reaction region are ionized. The chirped probe pulses now are able to interact with the molecular ions resulting in further fragmentation, which is the process of interest in this work. The relative yields of the major fragments as a function of the delay time between two pulses are shown in Figure 6. Clearly, our strategy to chirp the probe allowed us to better observe the picosecond modulation.

The results in Figure 6 show a fast feature observed around zero delay time with a longer decay time compared to the one observed for the TL–TL case. The increase in the relative yield

of benzoyl ions (m/z 105) and the decrease in the relative yield of phenyl ions (m/z 77) with time delay were observed with time constants of 19.4 ± 0.8 and 18.8 ± 1.2 ps, respectively. An interesting observation from this experiment is the oscillations observed for the ion yield of molecular ions, benzoyl ions, and phenyl ions within the first 3 ps, as can be seen in Figure 6. The period is determined to be 0.685 ± 0.015 ps, and fits to the data are given in the Supporting Information Figures S1–S3.

Pump (TL)–Probe (Chirped) on Partially Deuterated Acetophenone and Methyl-acetophenones. Pump–probe measurements were also carried out for d_3 -acetophenone and methyl-acetophenones using a TL pump pulse followed by a $+2500$ fs² chirped probe pulse. The yield of the benzoyl ion for which oscillations were observed is plotted with respect to the time delay between the pump (TL) and probe (chirped) pulses, as shown in Figure 7. The yield of benzoyl ion obtained from acetophenone molecules is also plotted as reference.

As can be seen in the short time scale (Figure 7, left), the period of the oscillation does not change between acetophenone and deuterated acetophenone. For the methyl benzoyl ions generated from methyl-acetophenones, a clear difference can be seen in the oscillations. The periods for *ortho*- and *para*-methyl acetophenone are 1.040 ± 0.30 and 1.033 ± 0.034 ps respectively, which is an approximately 53% longer period than that for the acetophenone molecules. On the other hand, no oscillations were observed for *meta*-methyl-acetophenone. The detailed analyses of the oscillations, including fits to the data, are given in the Supporting Information Figures S1–S3.

DISCUSSION

Photodissociation of Acetophenone. In all the experiments, a fast feature in the ion yields was observed when pump

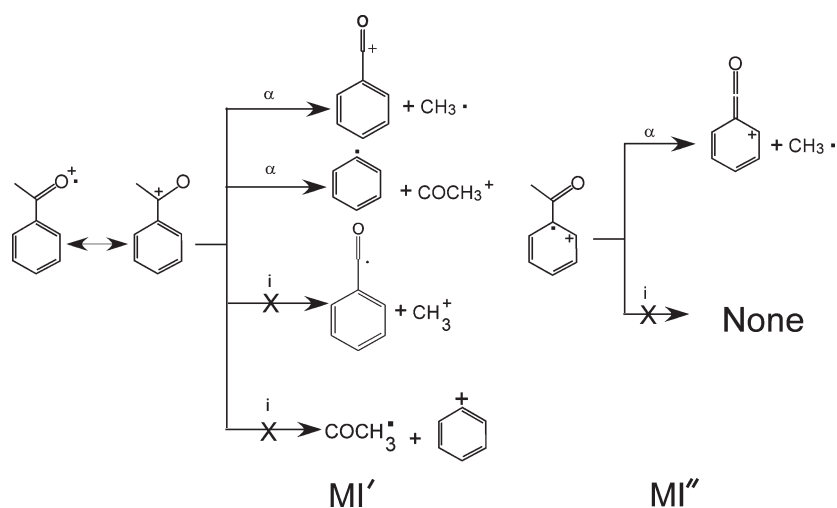


Figure 8. Structures of acetophenone molecular ions formed by losing an electron from the oxygen (MI') or from the benzene ring (MI''), and their major fragmentation pathways.

and probe pulses were overlapped in time. The temporal width of this feature was found to coincide with the cross correlation between the pump and probe pulses. In all the experiments, because the intensity of the pump TL pulses at the focus is 4×10^{15} W/cm², higher than the ionization threshold (I_{sat}) of acetophenone molecules ($\sim 10^{14}$ W/cm²), most of the molecules are field ionized. The appearance of the time zero feature is more likely due to the increase of the volume in which the laser intensity exceeds the ionization threshold I_{sat} .

The acetophenone radical cations can be formed by taking a nonbonding electron either from the carboxylic group oxygen (MI') or from the benzene ring (MI''), as illustrated in Figure 8. The most favored radical and charge sites in the molecular ion are assumed to arise from loss of the electron with lowest ionization energy in the molecule, which indicates the order of the electron loss should be according to the orbitals $n > \pi > \sigma$. Photoelectron spectroscopy measurements corroborate the source of the first electron as coming from the oxygen nonbonding orbitals.¹⁹ Thus, MI' is the most probable structure of the acetophenone molecular ion. When the probe pulse arrives, additional energy becomes available, MI' could undergo further fragmentation by α -cleavage (radical site initiated) or i -cleavage (charge site initiated). As can be seen from Figure 8, MI' can only undergo α -cleavage to form benzoyl cation ($C_6H_5CO^+$) and methyl radical ($CH_3\bullet$) or acylium cation (CH_3CO^+) and phenyl radical ($C_6H_5\bullet$). The bond dissociation energies are 0.82 and 2.02 eV,²⁰ respectively, suggesting the first channel (benzoyl cation and CH_3 neutral radical) is energetically more favorable. The yield of benzoyl cations compared to acylium cations confirms the energy favored pathway. The i -cleavage would form phenyl cation or methyl cations directly, however, both have higher formation energies.

Although less favorable, for acetophenone, loss of a π electron from the benzene ring to form MI'' could take place. As shown for MI'' , the only possible fragmentation channel is to form the benzoyl cation and methyl radical by α -cleavage. For the methyl substituted acetophenones, however, this pathway has been found to be dominant by photoelectron spectroscopy (see discussion below).¹⁹

The benzoyl cation could also absorb additional photons and fragment into CO and phenyl cation, as shown in Figure 9. The

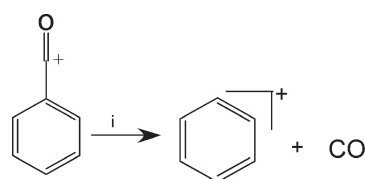


Figure 9. Fragmentation of the benzoyl cation.

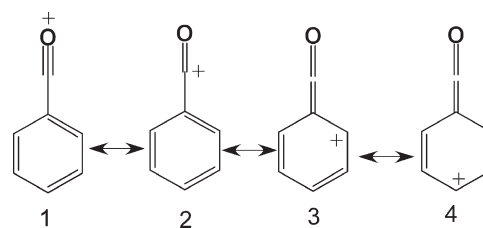


Figure 10. Resonance structures of benzoyl ion.

benzoyl ions have several resonance structures as shown in Figure 10. According to Bursey et al.²¹ resonance structure 1 has the lowest energy. In the fragmentation of acetophenone, benzoyl ions are the most abundant fragment observed. When these fragments absorb additional photons from the probe pulse they fragment into phenyl ions and CO. This is the main source of phenyl ions, and is supported by the data shown in Figure 5, in which the yield of benzoyl ions is found to mirror (opposite) the yield of phenyl ions. Note that the modulation in the yield of phenyl cations is out of phase from that of the benzoyl ions. On the other hand, benzoyl ions are likely to relax to resonant structure 1, which is more stable and less likely to absorb photons required for further fragmentation. As can be seen from Figure 6, the yield of benzoyl ion increases with a time constant of 20.0 ± 1.6 ps.

Another interesting result in this experiment is observed for methyl cations. Normally, because of the higher ionization potential (IP = 9.80 eV) compared to that of the benzoyl cations (6.80 eV), methyl cations are unlikely to be formed directly from the dissociation of the molecular ion. This is confirmed by the very low abundance of CH_3^+ (only 1%) obtained with a single

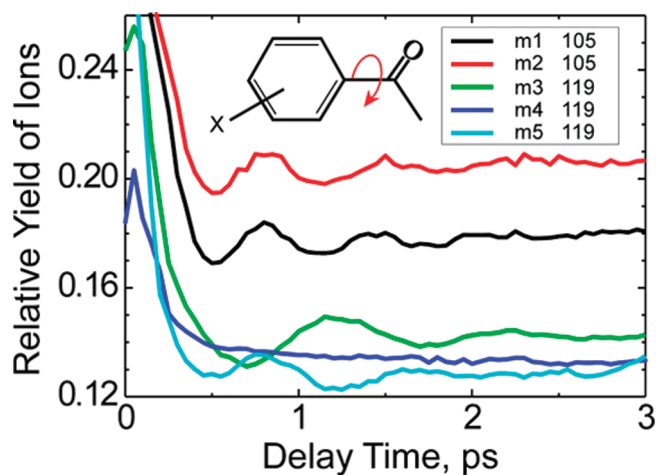


Figure 12. Zoom in of the oscillations shown in Figure 7. A schematic of the torsional vibration of the phenyl ring is shown on the right. Molecules are m1, acetophenone; m2, *d*₃-acetophenone; m3, 2-methyl-acetophenone; m4, 3-methyl-acetophenone; m5, 4-methyl-acetophenone.

Coulomb explosion through a doubly charged molecular ion, a process that is probably very fast, or from secondary ionization of methyl radicals. The slow ~ 20 ps rise rate of CH_3^+ , produced from molecular ion dissociation coincides with the appearance of benzoyl cation.

A closer look at the peak shapes of the fragment ions (figure not shown) reveals a contribution from doublet structures for COCH_3^+ (m/z 43), $\text{C}_6\text{H}_5\text{CO}_2^+$ (m/z 52.5), C_6H_5^+ (m/z 77), and CH_3^+ (m/z 15). This type of peak shape is known to arise from Coulomb explosion of multiply charged ions. Although Coulomb explosion will not be discussed in this paper because of its limited contribution, it would be interesting to study this process in detail in the future. The photodissociation pathways of acetophenone discussed above can be summarized by the ladder switching diagram shown in Figure 11.

Structural Dynamics. In this section we discuss the oscillations observed in the data; their analyses and fits to the data are given in the Supporting Information Figures S1–S3. The observed benzoyl ion yield from deuterated acetophenone has the same oscillation period as that of acetophenone suggesting that the process associated with loss of the methyl group cannot be responsible for the oscillations.

For methyl-substituted benzoyl ions generated from *ortho*- and *para*-methyl acetophenones, the oscillation periods were found to be 1.03 and 1.04 ps respectively, which are longer than the 0.685 ps found for acetophenone (see Figure 12 and Supporting Information Figures S2 and S3). We note that unlike acetophenone, for methyl substituted acetophenone, photoionization occurs primarily from the π -system.¹⁹ Additionally, the modulation of the *ortho* isomer was found to be out-of-phase with respect to acetophenone. The longer period implies that it is associated with an out-of-plane vibration, or a torsional motion. The methyl group in the *ortho* and *para* positions causes the period to increase by $\sim 50\%$; this is most likely due to the fact that methyl is an electron donating group and therefore decrease the barrier for rotation. The relative difference between *ortho* and *para* substitution in terms of the relative change in moment of inertia should cause a small change in the torsional period which is within our measurement error. No oscillations were observed

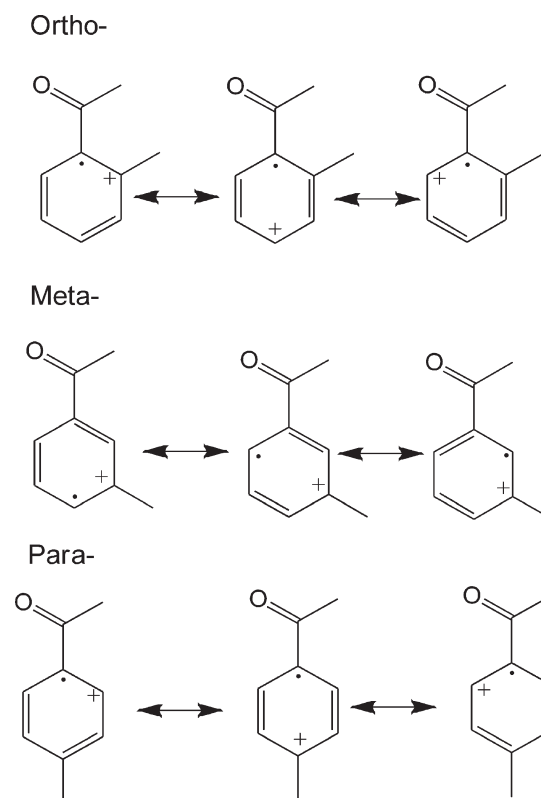


Figure 13. Resonance structures of the *ortho*, *meta*, and *para* isomers of acetophenone upon initial field ionization.

for the *meta*-methyl substituted acetophenone. We also noted that the yield of molecular ion for *meta*-methyl-acetophenone is 3 times higher than the *ortho* or *para* substituted isomers under laser photodissociation compared to electron ionization (see Figure 4).

Careful examination of the resonance structures of the molecular ions expected from methyl acetophenones provides information that can be used to explain the experimental observations (Figure 13). The resonance structures for *ortho* and *para* isomers lack a conjugate double bond between the carbonyl carbon and phenyl ring; therefore, the carbonyl group is able to rotate out of plane. For the *meta* isomer, however, all the resonance structures have the conjugated double bond structure; therefore, the carbonyl in the *meta*-methyl-acetophenone ions cannot rotate out of plane. The extended π system between the carbonyl group and the phenyl ring better stabilizes the radical cation of the *meta* isomer, which leads to a higher yield of molecular ion compared to the other isomers under femtosecond ionization. In the case of electron ionization, the radical ion is formed by removing an electron from oxygen. This leads to no difference between the yields among all isomers, under electron ionization.

It has been found that cyclic aromatic hydrocarbon ions lack electronic transitions at 800 nm.²² Therefore, when the carbonyl group rotates out of the plane with respect to the phenyl group, the unpaired electron is confined within the phenyl ring and is not likely to absorb additional 800 nm photons. This results in less fragmentation and more intact molecular or benzoyl ions. When the phenyl ring is in the same plane with the carbonyl group, the unpaired electron can be delocalized within the π -system including the CO double bond, increasing the probability

of absorbing additional 800 nm photons and resulting in fragmentation. This is why the modulation of benzoyl and phenyl ion yields is out of phase or all the molecules studied.

In the resonance structures of *ortho* and *para* methyl substituted isomers, the radical is shown to be on the tertiary carbon adjacent to the acetyl group (See Figure 13). The presence of this radical site allows for torsional motion about the C—C bond, and further fragmentation of the molecular ion to its respective benzoyl and methyl species. However, for the meta methyl isomer, the radical does not exist at the same site. Instead, conjugation is associated with all the resonance structures of this isomer. Thus, both torsional motion about the C—C bond and fragmentation are hindered, and more molecular ion is observed

Our experimental data is consistent with the torsional motion of the carbonyl group causing the modulation in the ion yields. This conclusion is supported by the microwave spectrum of acetophenone molecules²³ for which the torsional frequency for acetophenone was 47.9 cm⁻¹. This frequency corresponds to period of 696 fs, which is reasonably close to the oscillation in the yield of benzoyl ions observed in this experiment (0.685 ± 0.015 ps).

CONCLUSION

In this work, we investigated the time-resolved photodissociation of acetophenone using a pump—probe scheme. From the change of ion abundances with respect to the time delay between two pulses, we are able to elucidate a number of ladder climbing and ladder switching pathways and their time constants. It is likely that these processes explain why pulse duration plays a critical role in determining product ion distributions in laser control experiments involving shaped nonresonant laser pulses.¹ An interesting oscillation was observed for the yield of benzoyl ions. By examining deuterated acetophenone and methyl-substituted acetophenone isomers, we confirmed that the oscillations are caused by the torsional motion of the carbonyl group, indicating that conformational control of the chemical reactions can be achieved by controlling the delay between two pulses.

ASSOCIATED CONTENT

S Supporting Information. Fits to the time-resolved dynamics for all the species studied, the rationale for TL pump and chirped probe experiments, and analysis of volume effects. This information is available free of charge via the Internet at <http://pubs.acs.org>.

AUTHOR INFORMATION

Corresponding Author

* E-mail: dantus@msu.edu.

ACKNOWLEDGMENT

Funding for this research comes from an SISGR grant from the Department of Energy (DE-SC0002325), and is gratefully acknowledged. We would like to thank Professors Gavin Reid, Dan Jones, and James Jackson, and Drs. Misha Redko and Xiaoyong Li for their help in elucidating the complex radical and ion reaction pathways.

REFERENCES

(1) Lozovoy, V. V.; Zhu, X.; Gunaratne, T. C.; Harris, D. A.; Shane, J. C.; Dantus, M. *J. Phys. Chem. A* **2008**, *112*, 3789.

(2) Kosmidis, C.; Marshall, A.; Clark, A.; Deas, R. M.; Ledingham, K. W. D.; Singhal, R. P. *Rapid Commun. Mass Spectrom.* **1994**, *8*, 607.

(3) Ledingham, K. W. D.; Kilic, H. S.; Kosmidis, C.; Deas, R. M.; Marshall, A.; McCanny, T.; Singhal, R. P.; Langley, A. J.; Shaikh, W. *Rapid Commun. Mass Spectrom.* **1995**, *9*, 1522.

(4) Kosmidis, C.; Ledingham, K. W. D.; Kilic, H. S.; McCanny, T.; Singhal, R. P.; Langley, A. J.; Shaikh, W. *J. Phys. Chem. A* **1997**, *101*, 2264.

(5) Tasker, A. D.; Robson, L.; Ledingham, K. W. D.; McCanny, T.; Hankin, S. M.; McKenna, P.; Kosmidis, C.; Jaroszynski, D. A.; Jones, D. R. *J. Phys. Chem. A* **2002**, *106*, 4005.

(6) Shane, J. C.; Lozovoy, V. V.; Dantus, M. *J. Phys. Chem. A* **2006**, *110*, 11388.

(7) Rosker, M. J.; Dantus, M.; Zewail, A. H. *J. Chem. Phys.* **1988**, *89*, 6113.

(8) Dantus, M.; Rosker, M. J.; Zewail, A. H. *J. Chem. Phys.* **1988**, *89*, 6128.

(9) Dantus, M.; Rosker, M. J.; Zewail, A. H. *J. Chem. Phys.* **1987**, *87*, 2395.

(10) Yang, J. J.; Gobeli, D. A.; El-Sayed, M. A. *J. Phys. Chem.* **1985**, *89*, 3426.

(11) Szaflarski, D. M.; El-Sayed, M. A. *J. Phys. Chem.* **1988**, *92*, 2234.

(12) Pearson, B. J.; Weinacht, T. C. *Opt. Express* **2007**, *15*, 4385.

(13) Kotur, M.; Weinacht, T.; Pearson, B. J.; Matsika, S. *J. Chem. Phys.* **2009**, *130*.

(14) Greenfield, M.; McGrane, S. D.; Moore, D. S. *J. Phys. Chem. A* **2009**, *113*, 2333.

(15) Assion, A.; Baumart, T.; Bergt, M.; Brixner, T.; Kiefer, B.; Sayfried, V.; Strehle, M.; Gerber, G. *Science* **1998**, *282*, 919.

(16) Brif, C.; Chakrabarty, R.; Rabitz, H. *New J. Phys.* **2010**, *12*, 68.

(17) Coello, Y.; Lozovoy, V. V.; Gunaratne, T. C.; Xu, B. W.; Borukhovich, I.; Tseng, C. H.; Weinacht, T.; Dantus, M. *J. Opt. Soc. Am. B* **2008**, *25*, A140.

(18) Pastirk, I.; Resan, B.; Fry, A.; MacKay, J.; Dantus, M. *Optics Exp.* **2006**, *14*, 9537.

(19) Kobayashi, T.; Nakagura, S. *Bull. Chem. Soc. Jpn.* **1974**, *47* (10), 2563–2572.

(20) Anand, S.; Zamari, M. M.; Menkir, G.; et al. *J. Phys. Chem. A* **2004**, *108*, 3162–3165.

(21) Burse, M. M.; Kao, J. L.; Pedersen, L. *Org. Mass Spectrom.* **1975**, *10*, 38.

(22) Harada, H.; Shimizu, S.; Yatsuhashi, T.; Sakabe, S.; Izawa, Y.; Nakashima, N. *Chem. Phys. Lett.* **2001**, *342*, 563.

(23) Onda, M.; Kohama, Y.; Suga, K.; Yamaguchi, I. *J. Mol. Struct.* **1998**, *442*, 19.